U.S. DEPARTMENT OF THE INTERIOR

U.S. GEOLOGICAL SURVEY

# WHOLE-ROCK AND MINERAL CHEMICAL COMPOSITIONAL DATA FOR LOWER CRUSTAL AND UPPER MANTLE XENOLITHS FROM THE CIMA VOLCANIC FIELD, SAN BERNARDINO COUNTY, CALIFORNIA

by

H.G. Wilshire[1] and S.B. Mukasa[2]

Open-File Report 97-173



[1]345 Middlefield Road MS/975, Menlo Park, CA 94025
[2]The University of Michigan, Ann Arbor, MI 48109-1063

WHOLE-ROCK AND MINERAL CHEMICAL COMPOSITIONAL DATA FOR LOWER CRUSTAL AND UPPER MANTLE XENOLITHS FROM THE CIMA VOLCANIC FIELD, SAN BERNARDINO COUNTY, CALIFORNIA

## Introduction

This report provides major element chemical data on lower crustal and upper mantle xenoliths and their constituent minerals from the Cima volcanic field (CVF) selected for isotopic studies (Mukasa and Wilshire, submitted). The CVF has an unusually rich assemblage of lower crustal and upper mantle xenoliths, which have been intensively investigated (e.g., Wilshire and others, 1991; Parsons and others, 1995; McGuire and Wilshire, 1995; Wilshire and McGuire, 1996).

## Setting

Tertiary and Quaternary alkaline basalt fields, including the CVF, are scattered throughout the southern Basin and Range province (Fig. 1; Luedke and Smith, 1981). CVF volcanism began ~7.5 Ma (Turrin and others, 1985), continued until about 3 Ma, ceased for 2 m.y., and then resumed vigorously at about 1 Ma, continuing until perhaps several thousand years ago (Wells and others, 1991). There was no systematic migration of volcanism with time (Turrin and others, 1984), and small vents that probably differ in age by 10s to 100s of thousands of years coalesce.

The lava compositions are primarily hawaiites and alkali basalts that straddle the boundary between normative hypersthene and nepheline compositions (Wilshire and others, 1991). Most of the basalts have high $\varepsilon_{Nd}$ (7.6-9.3), low $^{87}Sr/^{86}Sr$ (0.7028-0.7040), and a restricted range of Pb isotopic compositions, interpreted to indicate a MORB source (Farmer and others, 1995). 100 $Mg/(Mg+Fe^{2+})$(cation %) values range from 40 to 62, and normative values of 100 an/(an+ab) range from 29 to 54, indicating generally evolved compositions. Proportionally more of the basalts older than 3 m.y. are hy-normative than ones younger than 1 m.y. The basalts are sparsely porphyritic with olivine and plagioclase phenocrysts, and uncommonly with clinopyroxene phenocrysts, in a cryptocrystalline, intergranular, or, rarely, subophitic groundmass of olivine, clinopyroxene, plagioclase, and opaque oxides. The olivine and clinopyroxene phenocrysts show normal zoning. Plagioclase phenocrysts show weak to strong oscillatory zoning in some basalts and normal zoning in others.

## Megacrysts and Xenoliths in CVF Basalts

Scattered broken feldspar and pyroxene crystals (megacrysts) and small two or three grain lithic fragments are present in almost all Cima lavas. Spinel and orthopyroxene megacrysts have opaque oxide and olivine + glass reaction rims, respectively; plagioclase megacrysts are resorbed and sieved with glass inside reverse-zoned overgrowths. Apatite and kaersutite megacrysts are uncommon. Xenocrysts of strongly resorbed microcline and quartz with clinopyroxene reaction rims are present in some basalts. Several cinder cones and flows contain abundant mafic and ultramafic xenoliths as much as 50 cm across (Wilshire and others, 1991).

Mafic and ultramafic xenoliths from the CVF are divided into four groups (modified from Wilshire and others, 1991): (1) Cr-diopside group, represented by peridotite, websterite, and phlogopite ± pargasite clinopyroxenite; (2) "green-pyroxene" group, consisting of magnesian websterite, 2-pyroxene gabbro, and 2-pyroxene microgabbro; (3) Al-augite group, consisting of Fe-rich websterite, clinopyroxenite, clinopyroxene gabbro, and clinopyroxene microgabbro; and (4) hornblendite ± plagioclase ± phlogopite that typically forms veins in rocks of the Cr-

diopside group; these veins are believed to have been derived from amphibole-bearing members of either the green-pyroxene or Al-augite groups or both. All green-pyroxene and Al-augite group rock types occur as dikes in Cr-diopside group rock types.

Cr-diopside group xenoliths have metamorphic textures, or hybrid textures where a metamorphic host was infiltrated by basaltic melt. About 40% of infiltrated peridotites were deformed and recrystallized after infiltration (Wilshire, 1990; Wilshire and others, 1991). Green-pyroxene and Al-augite group rocks have igneous textures. Some gabbros are weakly deformed, and others are texturally heterogeneous with irregular fine-grained domains of well-developed triple-junction intergrowths of plagioclase and pyroxenes; these may have been partly recrystallized. The hornblendites have allotriomorphic granular textures of either igneous or metamorphic origin.

## Whole-Rock and Mineral Major Element Compositions

Major elements. Table 1 gives major element compositions of xenoliths and basalt samples, and selected oxides and elements are plotted on MgO variation diagrams in Figure 2 [additional data used in plots from Wilshire and others, 1991 Table 2, Fig. 6, and Farmer and others, 1995, Tables 1-2, Fig. 4]. Whole rock MgO varies from ~3.5 to 43 wt%, with a gap of ~10 wt% MgO between peridotites and pyroxenites of the Cr-diopside group. MgO of the green-pyroxene group xenoliths overlaps that of the Cr-diopside pyroxenites and Al-augite group gabbros and pyroxenites. Basalts overlap slightly the low MgO members of the green-pyroxene and Al-augite groups. The major elements either show no correlation with MgO ($SiO_2$, FeO, CaO) or show scattered nonlinear inverse correlations ($Al_2O_3$, $Na_2O+K_2O$, $TiO_2$) (Figure 2a-c). The latter oxides show slight to moderate increases with decreasing MgO from peridotite through Cr-diopside pyroxenite to green-pyroxene and Al-augite group gabbros and pyroxenites, and then generally steep increases through the basalts. The unclassified plagioclase hornblendite (Ci-1-402) commonly is isolated from other rock types. Infiltrated peridotites, having lower MgO contents than unaltered peridotites, partially fill the gap between unaltered peridotite and Cr-diopside pyroxenites.

Compatible trace elements (data given by Mukasa and Wilshire, submitted) such as Ni and Cr show scattered positive correlations with MgO, more strongly with Ni than with Cr (Figure 2d-e); infiltration of peridotite by melts that crystallized amphibole caused a much sharper reduction in Cr than did those infiltrated by melts that crystallized plagioclase, but had no effect on Ni compared to a moderate reduction of Ni in the plagioclase peridotite. The green-pyroxene group olivine-rich gabbro (Ci-6-2) is isolated from other rock types on a Cr-MgO plot.

Incompatible trace elements (data given by Mukasa and Wilshire, submitted) such as Sr and Hf (Figure 2f-g) show slight to moderate inverse correlations with MgO. The Cr-diopside group pyroxenites plot with the green-pyroxene and Al-augite group rocks on the Hf and Sr diagrams. The plagioclase hornblendite is completely isolated on the Sr plot, and clustered with the Cr-diopside group pyroxenites on the Hf plot. On the Hf plot there is a gap between the basalts and the gabbros and pyroxenites of the green-pyroxene and Al-augite groups, but not on the Sr plot.

A major part of the whole rock compositional range for the Cr-diopside group is produced by the pyroxenites, which represent dikes in the peridotite. Lesser effects resulted from infiltration of the peridotites. Variations in whole-rock compositions of the igneous rock groups are controlled principally by the abundance and type of pyroxene, and thus probably by cumulus processes. Gabbros of both the green-pyroxene and Al-augite groups typically are rich in pyroxene. Low $SiO_2$, and high CaO, $Al_2O_3$, $TiO_2$, and FeO* in clinopyroxene of the Al-

augite group rocks is reflected in whole-rock compositions, and by common presence of *ne* in their norms. The abundance of orthopyroxene in green-pyroxene group rocks is reflected by relatively high $SiO_2$ and low $Al_2O_3$, CaO, and $TiO_2$ in whole rock compositions, and by high *hy* and, in some, *q* in their norms.

## Mineral Compositions

Mineral compositions determined by electron microprobe analysis are presented in Table 2, and on diagrams augmented with data reported by Wilshire and others (1991) in Figure 3. In general, the observed variations for the Cima Cr-diopside, green-pyroxene, and Al-augite xenolith groups are similar to those reported from other Basin and Range localities (Wilshire and others, 1988, 1991). Fe-Mg variations in olivine and orthopyroxene (Figure 3a, b) have two clusters, one of the "unaltered" Cr-diopside group rocks and infiltrated peridotite, and the other comprising green-pyroxene and Al-augite group rocks. Internal inverse correlations of MgO and FeO are evident. Fe-Mg variations in clinopyroxenes (Figure 3c) also have two clusters, but clinopyroxenes of green-pyroxene group rocks are split between the two clusters; internal inverse correlation of MgO and FeO in clinopyroxene is more scattered in the cluster including peridotites, and not present in the cluster containing Al-augite group rocks. Orthopyroxene shows inverse correlation of $Cr_2O_3$ and $Al_2O_3$ in separate trends for unaltered peridotite and rocks of the green pyroxene group (Figure 3d). Clinopyroxene shows little variation in $Cr_2O_3$ vs $Al_2O_3$, except for substantial scatter at the low $Cr_2O_3$ end (Figure 3e).

## Acknowledgments

We are indebted to Anne McGuire, Charles Meyer and Jane Nielson, USGS for microprobe analyses, and Michael Clynne, USGS for review of the manuscript.

## Appendix—Petrologic Descriptions of Samples

Samples were chosen for isotopic analysis to represent as wide a range of rock types present as possible. Modal compositions are given in Table 3. Mineral separates were made from all medium- and coarse-grained rocks while microgabbros were processed only as whole-rock powders.

### *Cr-diopside group.*

*Ki-5-31. Lherzolite.* Allotriomorphic-granular texture; no grain deformation, exsolution, or twinning; ~0.5-1.0 mm grain size. 1-2% red-brown spinel molded on grain boundaries and inclusions in all silicate minerals. Locally feldspathic, plagioclase in textural equilibrium. Mineral separates taken from nonfeldspathic part of xenolith.

*Ki-5-17. Websterite.* Allotriomorphic-granular texture; no grain deformation, exsolution, or twinning; ~0.5-2.0 mm grain size. ~1% interstitial brown glass.

*Ci-1-544A. Amphibole, Phlogopite orthopyroxene-poor websterite.* Allotriomorphic-granular to porphyroclastic, inequigranular texture; distinct bands to ~1 cm wide have porphyroclastic texture with mosaic matrix; amphibole and mica occur as small anhedral grains in the recrystallized matrix and as larger grains intergrown with pyroxene in the allotriomorphic-granular parts; no grain deformation, exsolution, or twinning; <0.5-2.5 mm grain size. Amphibole and phlogopite interstitial, in textural equilibrium with anhydrous silicates. Hydrous minerals marginally broken down to mats of oriented acicular crystals and cryptocrystalline material.

### *Metasomatized Cr-diopside subgroup.*

*Ci-1-281. Amphibole-bearing lherzolite.* Strongly foliated tectonite texture with some recrystallized tabular olivine grains; all minerals are elongate in the foliation, including amphibole, which is in textural equilibrium with olivine and pyroxenes; weak to moderate deformation bands in olivine and orthopyroxene, no exsolution or twinning; typical grain size ~2-3 mm. Amphibole marginally melted to brown vesicular glass with tiny titanaugite and skeletal plagioclase quench crystals.

*Ki-5-139. Plagioclase-bearing lherzolite.* Porphyroclastic with strongly foliated tectonite matrix texture, which includes plagioclase in textural equilibrium with olivine and pyroxenes; low degree of partial melting at edges of clinopyroxene; plagioclase crystallized from melt zones is zoned; weak deformation banding in olivine, exsolution lamellae in large relict pyroxene grains; matrix grain size ~0.5-2.0 mm, relict grains to 7 mm.

### *Green-pyroxene group.*

*Ki-5-229. Feldspathic websterite.* Hypidiomorphic-granular, inequigranular texture; orthopyroxene prisms have core zones with abundant blebs of exsolved clinopyroxene; clinopyroxenes have patchy zones of exsolved orthopyroxene blebs, some with "fingerprint" texture; clinopyroxenes complexly twinned. Plagioclase occurs as interstitial plates with enclosed small pyroxene euhedra. Small amount of opaque or vesicular brown glass, especially surrounding sparse primary opaque oxide grains; brown glass has plagioclase and olivine quench crystals; grain size <0.5 mm to 3.0 mm.

*Ki-5-47. 2-pyroxene gabbro.* Hypidiomorphic-granular, equigranular texture; pyroxenes occur in loose clusters among plagioclase laths; both pyroxenes have very fine blebby exsolution, and show complex intergrowths; plagioclase has weak oscillatory zoning, deep corrosion of some inner zones; moderate amount of interstitial opaque vesicular glass; typical grain size 3.0-4.0 mm.

*Ci-1-265. 2-pyroxene gabbro.* Hypidiomorphic-granular, inequigranular texture; plagioclase anhedral to subhedral, patchy extinction, very weak if any zoning; clinopyroxenes with abundant blebs and lamellae of exsolved orthopyroxene are coarse, wormy grains that enclose irregular blebs of plagioclase; some bead-like trains enclosed in plagioclase; orthopyroxenes have a very fine lamellar texture and irregularly distributed exsolution blebs; typical grain size 5.0-6.0 mm.

*Ci-6-2.* Rock consists of clusters (xenoliths?) 1-4 mm across of anhedral clino- and orthopyroxene intergrowths enclosed in a hypidiomorphic-granular intergrowth of coarse plagioclase enclosing or intergrown with olivine; the clinopyroxenes have "fingerprint" exsolution and complex twinning, whereas the orthopyroxenes have abundant exsolved blebs of clinopyroxene; in some sections, olivine occurs as clusters of grains with common orientation enclosed in large plates of plagioclase, and in others as coarse bladed intergrowths of prismatic olivine and plagioclase; grain size in the olivine-plagioclase areas is > 1 cm.

*Ci-1-2C. 2-pyroxene gabbro.* (Rock consists of coarse gabbro and microgabbro; analyzed part is the coarse gabbro). Hypidiomorphic-granular, equigranular texture; plagioclase laths and plates have patchy extinction, weak deformation; clinopyroxenes have complex patchy distribution of "fingerprint" exsolution and irregular internal zones of varying optical orientation; orthopyroxene has blebby exsolution and patchy extinction. Typical grain size 3.0-4.0 mm.

*Ci-1-11A. 2-pyroxene microgabbro.* Hypidiomorphic-granular texture; plagioclase plates ~1-3 mm across with weak oscillatory zoning enclose many small clinopyroxene anhedra and orthopyroxene prisms; pyroxenes have blebby to lamellar exsolution. The larger clinopyroxene grains (~0.5 mm) may be subhedral, are normally zoned, and contain rounded inclusions of orthopyroxene. Both the xenolith and the host basalt have fairly abundant cavities lined with botryoidal growths of dusky microcrystalline carbonate(?).

***Al-augite group.***

*Ci-9-80. Clinopyroxenite.* Allotriomorphic-granular, moderately inequigranular; no exsolution or twinning; abundant deep green spinel in grains as large as the pyroxenes, but with edges complexly molded along boundaries of adjacent pyroxenes; minor interstitial plagioclase; grain size ~1.0-4.0 mm. The xenolith preserves remnants of gabbro dikes at both ends, from which small, irregular apophyses composed entirely of plagioclase penetrate the pyroxenite; the analyzed minerals include plagioclase from these apophyses and pyroxene from the pyroxenite.

*Ki-2-9. Clinopyroxenite.* Allotriomorphic-granular, inequigranular; large clinopyroxene grains (to 14 mm) intergrown with mosaic of smaller grains; no exsolution or twinning; abundant opaque spinels, larger grains intergrown with larger clinopyroxenes.

*Ki-2-28. Single-pyroxene gabbro.* Allotriomorphic-granular, inequigranular texture; very sparse orthopyroxene exsolution lamellae in clinopyroxene; all minerals unzoned, undeformed; abundant deep green spinel, sparse olivine; grain size ~1.5-9.0 mm.

*Ki-5-88. Olivine microgabbro.* Slightly porphyritic with olivine phenocrysts in groundmass of plagioclase laths and equigranular clinopyroxene; larger pyroxenes have weak exsolution; interstitial opaque vesicular glass; grain size of groundmass ~0.5-1.0 mm.

*Ki-5-241. Olivine microgabbro* (rock consists of even-grained hypidiomorphic-granular olivine gabbro and microgabbro; analyzed part is the microgabbro). Allotriomorphic granular texture; equigranular plagioclase and clinopyroxene intergrown with very loose networks of optically continuous olivine to 3 mm across; plagioclase has three zones: a resorbed core and an intermediate zone whose outer part is normally zoned to the grain edge; clinopyroxenes are normally zoned; grain size ~0.2-0.7 mm.

***Unclassified.***

*Ci-1-402.* The analyzed sample is amphibole from a 1.5 cm-thick dike in porphyroclastic foliated lherzolite. The dike consists dominantly of interlocking pale brown pargasite grains to 1 cm across, with sparse small apatite inclusions, intergrown with clusters of smaller plagioclase grains. Small fragments of peridotite are enclosed in the dike; limited infiltration of the peridotite produced a small amount of interstitial amphibole grains within about 1 cm of the dike, and possible reaction rims on spinel grains farther from the contact; some infiltration is in the form of discontinuous amphibole apophyses to about 8 mm long; the amphiboles are marginally melted to brown glass with quench pyroxene, olivine, and plagioclase; similar rims on spinels, rarely with ragged remnants of amphibole, suggest melting of amphibole reaction rims on the spinels.

***Megacrysts.***

*Ci-9; Ci-7-4.* One sample each of plagioclase and amphibole megacrysts were analyzed. Plagioclase megacrysts are very common in Cima lavas and pyroclastics, whereas amphibole megacrysts are rare. The plagioclase sample, Ci-9, is the largest (8 cm across) such megacryst found at Cima.

## References


Farmer, G.L., Glazner, A.F., Wilshire, H.G., Wooden, J.L., Pickthorn, W.J., and Katz, M., Origin of late Cenozoic basalts at the Cima volcanic field, Mojave Desert, California: *J. Geophys. Res., 100*, 8399-8415, 1995.

Luedke, R.G. and Smith, R.L., 1981, Map showing distribution, composition, and age of late Cenozoic volcanic centers in California and Nevada: U.S. Geological Survey, Miscellaneous Investigations Series, Map I-1091-C, 1:1,000,000.

McGuire, A.V. and Wilshire, H.G., 1995, Compositional data on partial melt products in upper mantle and lower crustal xenoliths and their host basaltic rocks, world localities and Cima volcanic field, San Bernardino County, California: U.S. Geological Survey Open-file Report 95-585, 76 p.

Mukasa, S.B. and Wilshire, H.G., Isotopic and trace element compositions of upper mantle and lower crustal xenoliths, Cima volcanic field, California—Implications for evolution of the subcontinental lithospheric mantle, Journal of Geophysical Research, submitted.

Parsons, Tom, Christensen, N.I., and Wilshire, H.G., 1995, Velocities of southern Basin and Range xenoliths—Insights on the nature of lower crustal reflectivity and composition: Geology, v. 23, p. 129-132.

Turrin, B.D., Dohrenwend, J.C., Wells, S.G., and McFadden, L.D., 1984, Geochronology and eruptive history of the Cima volcanic field, eastern Mojave Desert, California, *in* Dohrenwend, J.C. (ed.) Surficial geology of the eastern Mojave Desert, California: Guidebook Geological Society of America, 1984 Annual Meeting, Field trip 14, p. 88-100.

Wells, S.G., McFadden, L.D., and Olinger, C.T., 1991, Use of cosmogenic $^{3}He$ & $^{21}Ne$ to understand desert pavement formation: Geological Society of America, Abstracts with Programs, v. 23, p. 206.

Wilshire, H.G., 1990, Lithology and evolution of the crust-mantle boundary region in the southern Basin and Range province: Journal of Geophysical Research, v. 95, p. 649-665.

Wilshire, H.G., and A.V. McGuire, Magmatic infiltration and melting in the lower crust and upper mantle beneath the Cima volcanic field, *California: Contrib. Mineral. Petrol., 123*, 358-374, 1996.

Wilshire, H.G., McGuire, A.V., Noller, J.S., and Turrin, B.D., Petrology of lower crustal and upper mantle xenoliths from the Cima volcanic field, California: *Jour. Petrol.., 32*, 169-200, 1991.

Wilshire, H.G., Meyer, C.E., Nakata, J.K., Calk, L.C., Shervais, J.W., Nielson, J.E., and Schwarzman, E.C., 1988, Mafic and ultramafic xenoliths from volcanic rocks of the western United States: U.S. Geological Survey Professional Paper 1443, 179 p.

Figure Captions

Figure 1. Map showing locations of Cima and selected other western U. S. and Mexican xenolith localities of the Basin and Range province, Rio Grande rift, and Transition Zone of the Colorado Plateau.

Figure 2: Cima whole-rock MgO variation versus (**a**) $Al_2O_3$, (**b**) total alkalis ($Na_2O + K_2O$), (**c**) $TiO_2$, (**d**) Ni, (**e**) Cr, (**f**) Sr, and (**g**) Hf for xenoliths and their Cenozoic basaltic host rocks. Note the nonlinear inverse correlations in a, b, c, f and g, nonlinear positive correlations in d and e, the gap in MgO between peridotites and pyroxenites of the Cr-diopside group, and the overlap in MgO between the green pyroxene and Al-augite groups as well as the pyroxenites of the Cr-diopside group.

Figure 3: Mineral variation diagrams for the different rock groups based on electron microprobe data. (**a**) - (**c**) show MgO versus total Fe as FeO for olivine, orthopyroxene and clinopyroxene, respectively, while (**d**) and (**e**) show $Cr_2O_3$ versus $Al_2O_3$ in orthopyroxene and clinopyroxene.

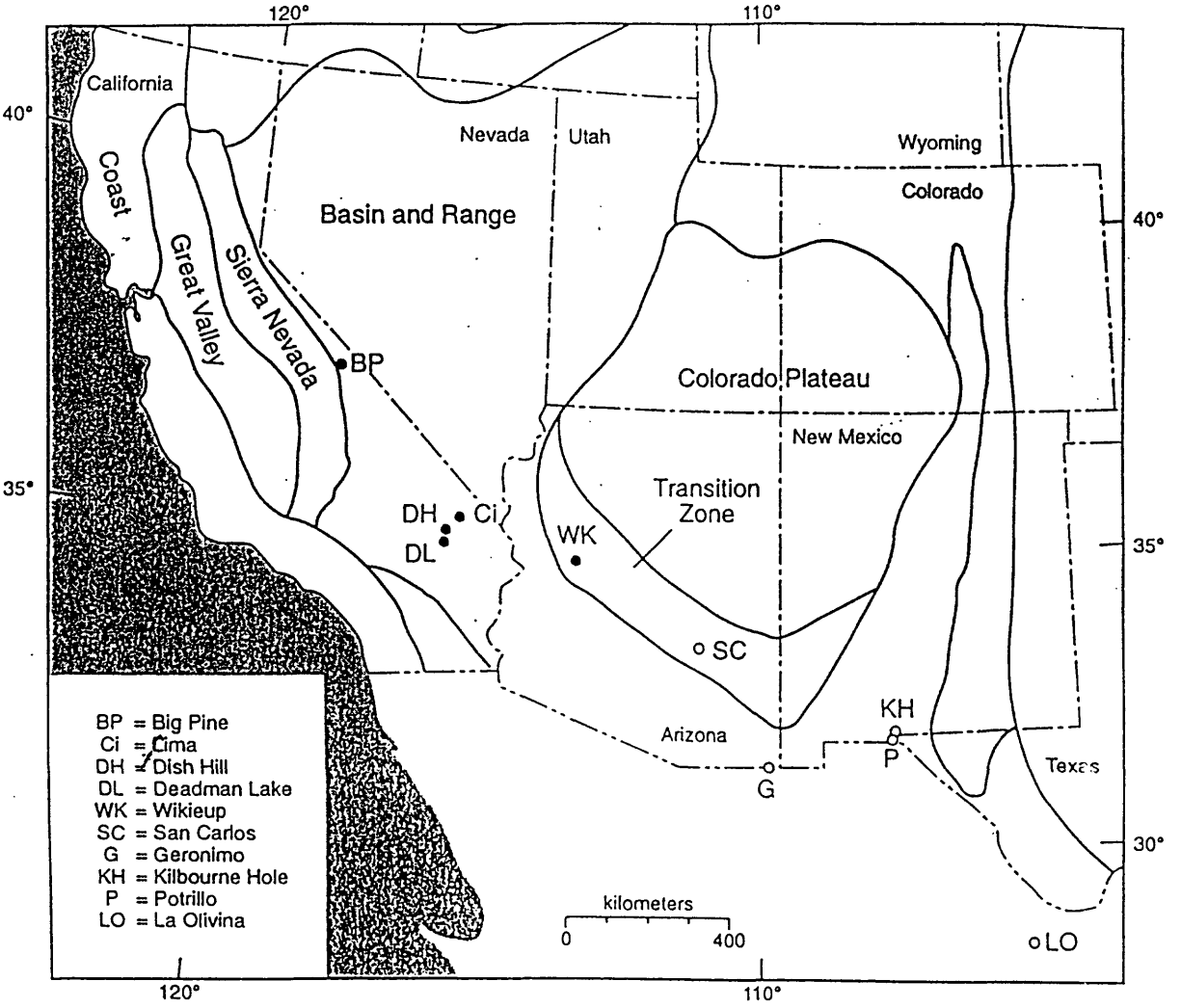
120°
110°
40°
35°
30°
California
Nevada
Utah
Wyoming
Colorado
Coast
Great Valley
Sierra Nevada
Basin and Range
Colorado Plateau
New Mexico
Transition Zone
Arizona
Texas
BP
DH
Ci
DL
WK
SC
KH
P
G
LO
BP = Big Pine
Ci = Cima
DH = Dish Hill
DL = Deadman Lake
WK = Wikieup
SC = San Carlos
G = Geronimo
KH = Kilbourne Hole
P = Potrillo
LO = La Olivina
kilometers
0
400

Figure 1.

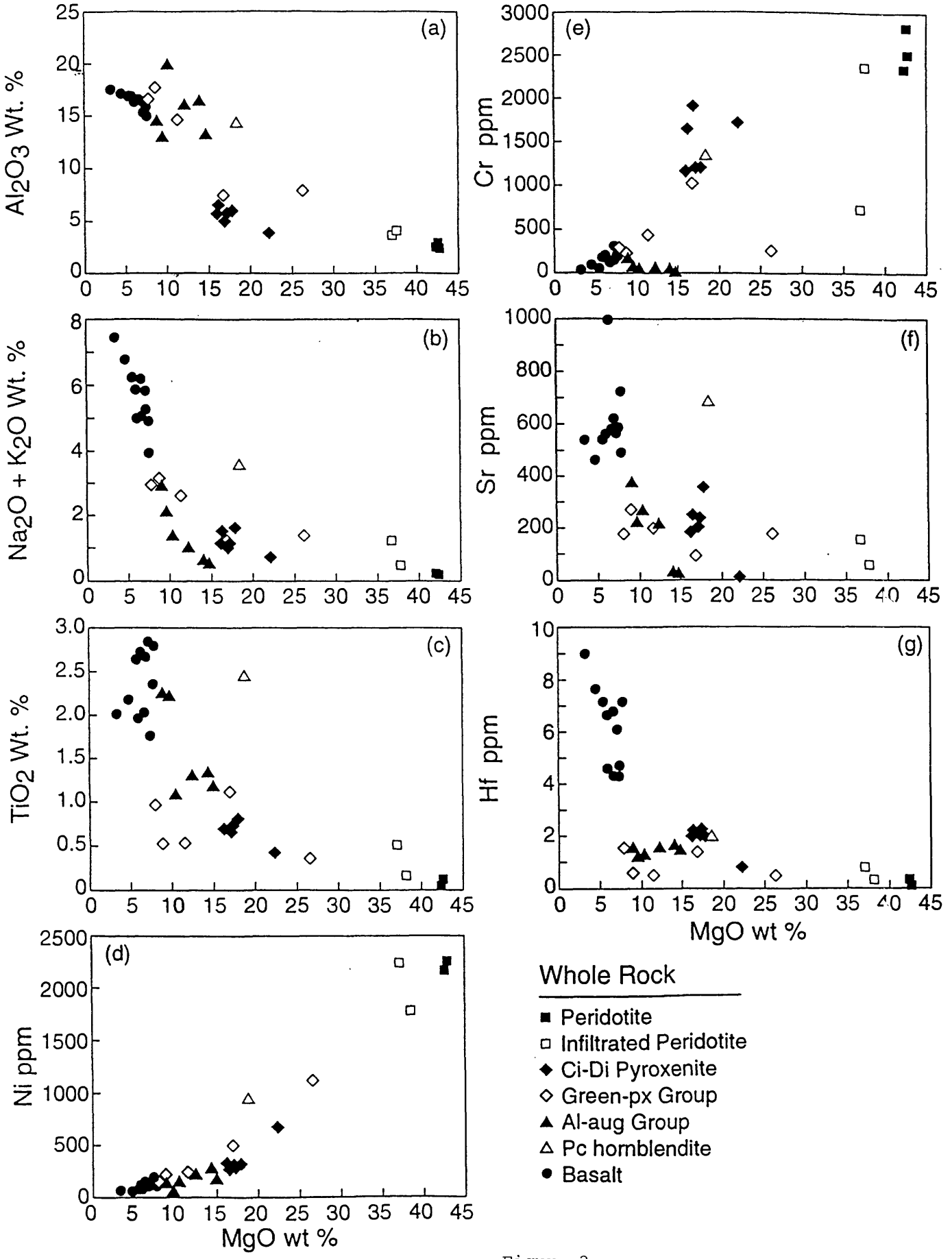
(a)
$Al_2O_3$ Wt. %
(b)
$Na_2O + K_2O$ Wt. %
(c)
$TiO_2$ Wt. %
(d)
Ni ppm
MgO wt %
(e)
Cr ppm
(f)
Sr ppm
(g)
Hf ppm
MgO wt %
Whole Rock
Peridotite
Infiltrated Peridotite
Ci-Di Pyroxenite
Green-px Group
Al-aug Group
Pc hornblendite
Basalt

Figure 2

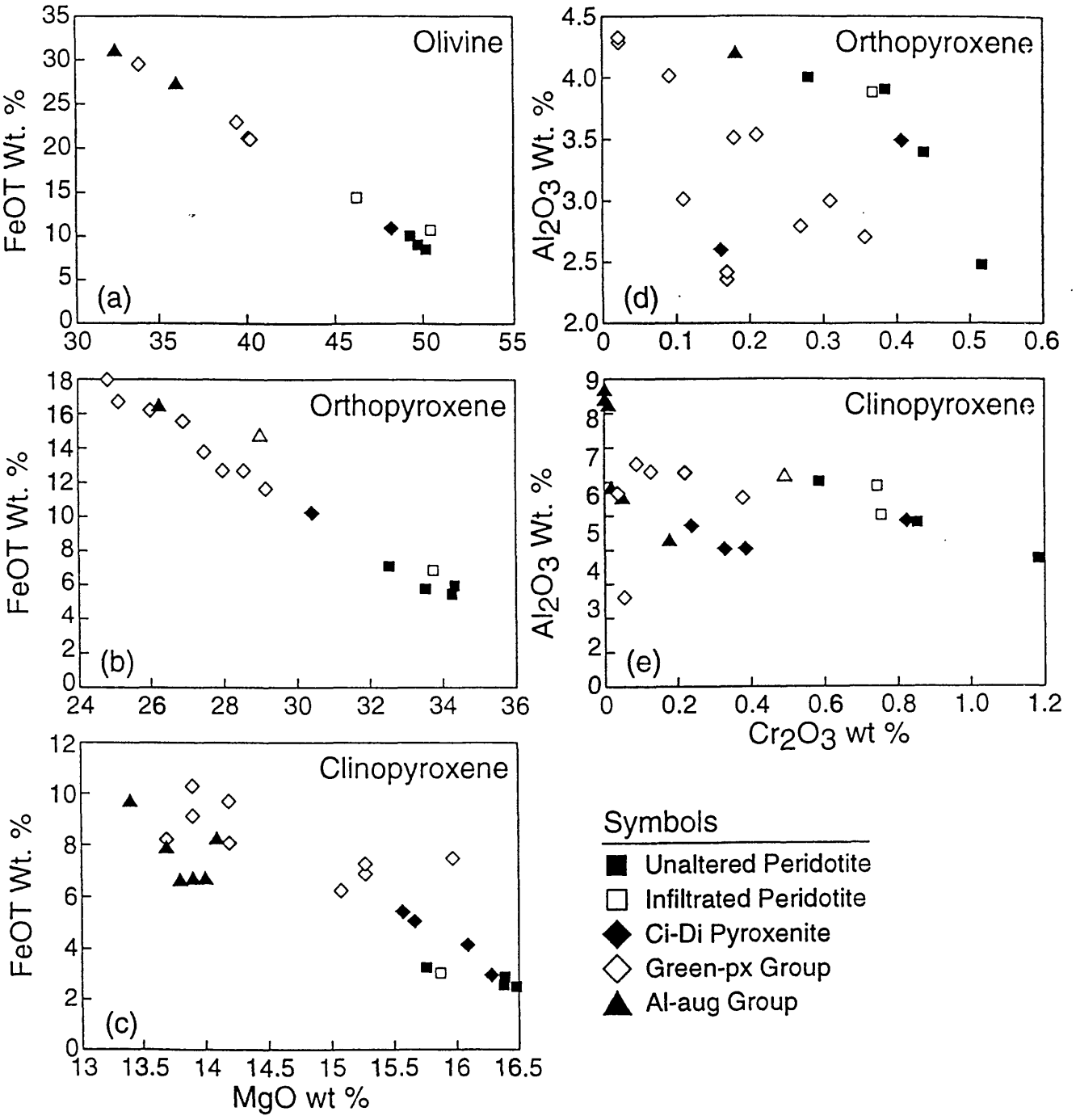
Olivine
(a)
FeOT Wt. %
Orthopyroxene
(b)
FeOT Wt. %
Clinopyroxene
(c)
FeOT Wt. %
MgO wt %
Orthopyroxene
(d)
Al2O3 Wt. %
Clinopyroxene
(e)
Al2O3 Wt. %
Cr2O3 wt %
Symbols
Unaltered Peridotite
Infiltrated Peridotite
Ci-Di Pyroxenite
Green-px Group
Al-aug Group

Figure 3

TABLE 1. Whole rock major-element compositions of xenoliths

| Rock Group/ Sample No. | $SiO_2$ | $Al_2O_3$ | $Fe_2O_3$ | FeO | MgO | CaO | $Na_2O$ | $K_2O$ | $H_2O+$ | $H_2O-$ | $TiO_2$ | $P_2O_5$ | MnO | $CO_2$ | Total |
|---|---|---|---|---|---|---|---|---|---|---|---|---|---|---|---|
| **Cr-Diopside Group** | | | | | | | | | | | | | | | |
| Ki-5-17 | 53.0 | 3.9 | 1.3 | 5.7 | 22.2 | 12.5 | .63 | .10 | .12 | .00 | .38 | .07 | .16 | <.05 | 100.06 |
| Ki-5-31 | 44.6 | 2.60 | 1.18 | 6.78 | 42.3 | 2.37 | .22 | <.02 | <.01 | <.01 | .04 | <.05 | .13 | .03 | 100.25 |
| Ci-1-544A | 50.1 | 5.60 | 1.91 | 4.49 | 16.1 | 18.7 | .81 | .28 | .38 | .41 | .68 | <.05 | .14 | .02 | 99.62 |
| **Metasomatized Cr-Diopside** | | | | | | | | | | | | | | | |
| Ci-1-281 | 41.3 | 3.64 | .97 | 10.92 | 37.0 | 3.14 | .85 | .32 | .14 | .06 | .50 | .06 | .17 | .12 | 99.19 |
| Ki-5-139 | 45.2 | 3.97 | .85 | 7.56 | 38.1 | 3.01 | .41 | .03 | <.05 | .06 | .14 | .09 | .14 | .06 | 99.62 |
| **Green-Pyroxene Group** | | | | | | | | | | | | | | | |
| Ki-5-47 | 51.5 | 16.5 | 1.3 | 6.5 | 7.8 | 11.0 | 2.7 | .26 | .77 | .06 | .96 | .14 | .13 | .25 | 99.87 |
| Ci-1-265 | 53.3 | 17.5 | 2.08 | 4.13 | 8.79 | 10.6 | 3.00 | .15 | .05 | .08 | .49 | <.05 | .10 | .11 | 100.38 |
| Ci-6-2 | 44.5 | 7.89 | 1.30 | 12.54 | 26.4 | 5.94 | 1.23 | .08 | .04 | .05 | .34 | <.05 | .16 | <.01 | 100.47 |
| Ci-1-2C | 52.2 | 14.7 | 3.65 | 3.33 | 11.4 | 11.7 | 2.44 | .13 | .09 | .04 | .53 | <.05 | .11 | .14 | 100.46 |
| Ci-1-11A | 49.7 | 7.22 | 4.81 | 6.74 | 16.8 | 11.6 | 1.08 | .11 | .14 | .04 | 1.11 | .05 | .18 | 1.08 | 100.66 |
| **Al-augite Group** | | | | | | | | | | | | | | | |
| Ki-2-9 | 43.6 | 13.3 | 3.83 | 4.20 | 14.7 | 17.9 | .64 | .02 | .08 | .06 | 1.18 | <.05 | .15 | .01 | 99.67 |
| Ci-9-80 | 39.9 | 16.6 | 6.40 | 3.81 | 14.0 | 16.8 | .67 | .07 | .45 | .31 | 1.34 | <.05 | .16 | .49 | 101.00 |
| Ci-9-80-1 | 42.5 | 16.2 | 4.85 | 3.86 | 12.2 | 16.4 | 1.03 | .14 | .43 | .20 | 1.31 | .05 | .15 | .05 | 99.37 |
| Ki-2-28 | 42.87 | 20.16 | 4.70 | 3.38 | 10.28 | 15.95 | 1.36 | .10 | .03 | .07 | 1.09 | .04 | .12 | .02 | 100.12 |
| Ki-5-88 | 42.8 | 13.1 | 8.1 | 9.1 | 9.53 | 11.9 | 1.99 | .17 | .23 | .14 | 2.21 | .07 | .14 | .22 | 99.70 |
| Ki-5-241 | 47.3 | 14.5 | 4.3 | 7.6 | 8.85 | 11.2 | 2.72 | .25 | .10 | .25 | 2.25 | .09 | .17 | .24 | 99.82 |
| **Unclassified** | | | | | | | | | | | | | | | |
| Ci-1-402 | 43.0 | 14.4 | 2.06 | 2.91 | 18.5 | 10.8 | 2.56 | 1.08 | 1.18 | .06 | 2.46 | .09 | .06 | .03 | 99.19 |
| **Basalt Host Rock** | | | | | | | | | | | | | | | |
| Ki-2-101 | 47.83 | 17.33 | 3.55 | 5.31 | 6.68 | 9.15 | 3.45 | 2.21 | .91 | .43 | 1.97 | .52 | .17 | .31 | 99.82 |
| Ki-5-101 | 47.75 | 16.33 | 2.96 | 7.19 | 6.83 | 8.81 | 3.88 | 1.73 | .53 | .10 | 2.40 | .58 | .17 | .48 | 99.74 |
| Ci-1-101 | 49.0 | 16.7 | 2.20 | 8.22 | 6.14 | 8.00 | 4.26 | 1.95 | .07 | .07 | 2.63 | .70 | .17 | .16 | 100.27 |
| Ci-6-1 | 48.4 | 16.5 | 3.00 | 6.99 | 7.13 | 8.65 | 4.04 | 1.82 | .38 | .20 | 2.85 | .68 | .17 | .13 | 99.80 |
| Ci-9-102 | 48.4 | 16.9 | 4.39 | 7.48 | 5.86 | 8.63 | 3.93 | 2.06 | .67 | .48 | 1.96 | .56 | .20 | .45 | 100.50 |

Ki-5-17 = websterite; Ki-5-31 = lherzolite; Ci-1-544 A = phlogopite, amphbole clinopyroxenite; Ci-1-281 = lherzolite infiltrated by amphibole, recrystallized; Ki-5-139 = lherzolite infiltrated by plagioclase, recrystallized; Ki-5-229 = websterite; Ki-5-47 = 2-pyroxene gabbro; Ci-1-265 = 2-pyroxene gabbro; Ci-6-2 = olivine-plagioclase-2-pyroxene rock; Ci-1-2C = 2-pyroxene gabbro; Ci-1-11A = 2 pyroxene microgabbro; Ki-2-9 = clinopyroxenite; Ci-9-80 = clinopyroxenite; Ci-9-80-1 = one-pyroxene gabbro; Ki-2-28 = one-pyroxene gabbro; Ki-5-88 = one pyroxene microgabbro; Ki-5-241 = one-pyroxene microgabbro; Ci-1-402 = hornblendite vein in Cr-diopside lherzolite.

TABLE 2. Microprobe data on megacrysts and xenoliths[1]

| Rock Group/ Sample No./ Mineral | $SiO_2$ | $Al_2O_3$ | Total Fe as FeO | MgO | CaO | $Na_2O$ | $K_2O$ | $TiO_2$ | MnO | $Cr_2O_3$ | NiO | $V_2O_3$ | Total |
|---|---|---|---|---|---|---|---|---|---|---|---|---|---|
| **Megacryst** | | | | | | | | | | | | | |
| Ci-7-4 | | | | | | | | | | | | | |
| Kaersutite | 39.39 | 14.51 | 14.66 | 10.63 | 11.10 | 2.82 | 1.13 | 5.29 | 0.21 | | | | 99.74 |
| Ci-9 | | | | | | | | | | | | | |
| Plagioclase | 60.60 | 24.60 | 0.16 | 0.01 | 5.67 | 7.58 | 1.16 | 0.03 | 0.00 | | | | 99.81 |
| **Cr-diopside Group** | | | | | | | | | | | | | |
| Ki-5-17 | | | | | | | | | | | | | |
| Clinopyroxene | 52.15 | 3.97 | 4.19 | 16.10 | 21.71 | 0.80 | | 0.40 | 0.12 | 0.33 | 0.05 | | 99.82 |
| Ki-5-31 | | | | | | | | | | | | | |
| Clinopyroxene | 51.82 | 5.02 | 2.62 | 16.40 | 21.47 | 1.06 | | 0.17 | 0.09 | 0.76 | | | 99.41 |
| Orthopyroxene | 54.72 | 3.91 | 5.82 | 33.58 | 0.75 | 0.07 | | 0.06 | 0.15 | 0.39 | | | 99.45 |
| Olivine | 40.61 | | 9.04 | 49.49 | 0.07 | | | | 0.15 | | 0.38 | | 99.74 |
| Spinel | | 52.68 | 10.92 | 20.61 | | | | 0.05 | 0.15 | 13.93 | | | 98.33 |
| Ci-1-544A | | | | | | | | | | | | | |
| Clinopyroxene | 51.02 | 4.60 | 5.38 | 15.55 | 21.71 | 0.65 | | 0.42 | 0.14 | 0.24 | 0.04 | | 99.75 |
| **Metasomatized Cr-diopside Grp** | | | | | | | | | | | | | |
| Ci-1-281 | | | | | | | | | | | | | |
| Olivine | 40.00 | 0.01 | 14.20 | 46.10 | 0.09 | 0.00 | | 0.00 | 0.21 | 0.00 | 0.34 | | 100.95 |
| Pargasite | 41.10 | 15.16 | 5.80 | 15.88 | 11.26 | 2.66 | 1.39 | 2.10 | 0.08 | | | | 99.43 |
| Ki-5-139 | | | | | | | | | | | | | |
| Clinopyroxene | 51.91 | 5.81 | 3.04 | 15.88 | 20.93 | 0.91 | | 0.62 | 0.10 | 0.75 | | | 100.01 |
| Orthopyroxene | 56.12 | 3.89 | 6.77 | 33.79 | 0.77 | 0.06 | | 0.01 | 0.16 | 0.37 | 0.10 | | 102.13 |
| Olivine | 41.36 | | 10.76 | 50.22 | 0.07 | 0.01 | | 0.03 | 0.16 | 0.01 | 0.38 | | 103.02 |
| Spinel | 0.06 | 53.17 | 12.08 | 20.42 | 0.01 | | | 0.12 | 0.11 | 14.29 | 0.33 | | 100.60 |
| Plagioclase | 56.60 | 27.37 | 0.08 | 0.06 | 9.74 | 5.26 | 0.23 | | 0.03 | | | | 99.44 |
| **Green Pyroxene Group** | | | | | | | | | | | | | |
| Ki-5-229 | | | | | | | | | | | | | |
| Clinopyroxene | 49.33 | 6.20 | 8.22 | 13.72 | 20.11 | 0.79 | | 1.36 | 0.18 | 0.22 | | | 100.15 |
| Orthopyroxene | 52.59 | 3.54 | 16.09 | 26.04 | 1.33 | 0.06 | | 0.33 | 0.29 | 0.21 | | | 100.48 |
| Oxide | | 0.40 | 37.16 | 7.92 | 0.06 | | | 52.60 | 0.38 | 0.90 | | | 99.39 |
| Plagioclase | 54.24 | 29.05 | 0.23 | | 11.25 | 5.10 | 0.25 | | | | | | 100.12 |
| Ci-6-2 | | | | | | | | | | | | | |
| Clinopyroxene | 50.11 | 5.52 | 6.17 | 15.10 | 20.05 | 0.68 | | 1.08 | 0.14 | 0.38 | | | 99.23 |
| Orthopyroxene | 53.36 | 2.81 | 12.54 | 28.64 | 1.48 | 0.07 | | 0.42 | 0.23 | 0.27 | | | 99.81 |
| Olivine | 38.05 | | 20.95 | 39.94 | 0.07 | | | | 0.26 | | 0.25 | | 99.52 |
| Oxide | | 0.41 | 34.63 | 9.75 | 0.06 | | | 53.50 | 0.32 | 0.41 | | 0.38 | 99.48 |
| Plagioclase | 53.90 | 29.58 | 0.16 | | 11.64 | 4.92 | 0.26 | | | | | | 100.46 |
| Ki-5-47 | | | | | | | | | | | | | |
| Clinopyroxene | 51.77 | 2.62 | 10.27 | 13.86 | 20.43 | 0.53 | | 0.52 | 0.24 | 0.06 | | | 100.31 |
| Orthopyroxene | 53.35 | 2.36 | 16.60 | 25.09 | 2.29 | 0.06 | | 0.32 | 0.29 | 0.17 | | | 100.53 |
| Oxide | | 0.60 | 38.24 | 8.11 | 0.04 | | | 51.50 | 0.27 | 0.25 | | | 99.00 |
| Plagioclase | 54.02 | 28.69 | 0.23 | | 11.38 | 5.07 | 0.27 | | | | | | 99.66 |
| Ci-1-2C | | | | | | | | | | | | | |
| Clinopyroxene | 48.46 | 6.37 | 9.17 | 13.85 | 18.22 | 1.03 | | 1.29 | 0.20 | 0.09 | | | 98.68 |
| Orthopyroxene | 50.87 | 4.27 | 17.95 | 24.80 | 1.27 | 0.08 | | 0.46 | 0.33 | 0.02 | | | 100.05 |
| **Al-augite Group** | | | | | | | | | | | | | |
| Ci-9-80 | | | | | | | | | | | | | |
| Clinopyroxene | 48.97 | 8.30 | 6.78 | 13.95 | 20.07 | 0.81 | | 1.52 | 0.18 | 0.01 | | | 100.58 |
| Spinel | | 60.83 | 21.21 | 17.74 | | | | 0.47 | 0.15 | 0.04 | | | 100.44 |
| Ki-2-9 | | | | | | | | | | | | | |
| Clinopyroxene | 48.12 | 8.51 | 8.28 | 14.13 | 19.95 | 0.79 | 0.02 | 1.25 | 0.15 | | | | 101.20 |
| Ki-2-28 | | | | | | | | | | | | | |
| Clinopyroxene | 48.59 | 8.71 | 6.69 | 13.80 | 20.16 | 0.91 | | 1.38 | 0.16 | 0.00 | | | 100.39 |
| Spinel | | 61.27 | 21.04 | 17.54 | | | | 0.38 | 0.15 | 0.02 | | | 100.40 |
| Plagioclase | 52.83 | 30.13 | 0.21 | 0.07 | 12.39 | 4.51 | 0.32 | | | | | | 100.46 |
| Ki-5-241 | | | | | | | | | | | | | |
| Clinopyroxene | 48.98 | 5.80 | 9.77 | 13.39 | 18.91 | 0.83 | | 1.40 | 0.27 | 0.02 | | | 99.37 |
| Olivine | 35.71 | | 31.12 | 32.26 | 0.11 | | | | 0.48 | | 0.06 | | 99.74 |
| Oxide | | 0.34 | 42.28 | 5.65 | 0.02 | | | 50.10 | 0.49 | 0.13 | | | 99.02 |
| Oxide | | 5.77 | 66.06 | 4.32 | 0.03 | | | 18.32 | 0.40 | 0.72 | | | 95.63 |
| Oxide | | 2.78 | 57.44 | 4.47 | 0.04 | | | 30.06 | 0.46 | 0.92 | | | 96.16 |
| Plagioclase | 56.61 | 27.11 | 0.23 | | 9.27 | 6.14 | 0.36 | | | | | | 99.70 |
| **Unclassified** | | | | | | | | | | | | | |
| Ci-1-402 | | | | | | | | | | | | | |
| Pargasite | 42.07 | 15.47 | 4.43 | 18.72 | 11.17 | 2.95 | 1.16 | 2.59 | 0.04 | | | | 98.60 |

[1]Averages of 10 analyses. Samples identified in Table 1.

TABLE 3. Modal Compositions of Analyzed Xenoliths[1]

| Sample | Ol | Opx | Cpx | Spinel | Plag | Hbl ± Mica | Glass + Xls |
|---|---|---|---|---|---|---|---|
| Cr-diopside Group | | | | | | | |
| Ki-5-31 | 77 | 13 | 6 | 4 | | | |
| Ki-5-17 | 6 | 26 | 58 | | | | 10 |
| Ci-1-544A | | 4 | 77 | | | 5 | 14 |
| Metasomatized Cr-diopside Group | | | | | | | |
| Ci-1-281 | 68 | 4 | 1 | | | 9 | 18 |
| Ki-5-139 | 73 | 11 | 4 | 2 | 7 | | 3 |
| Green-pyroxene Group | | | | | | | |
| Ki-5-229 | | 14 | 59 | | 12 | | 15 |
| Ki-5-47 | | 10 | 26 | | 53 | | 11 |
| Ci-1-265 | | 15 | 17 | | 61 | | 7 |
| Ci-6-2 | 41 | 4 | 20 | tr | 35 | | tr |
| Ci-1-2C | | 1 | 28 | 1 | 48 | | 22 |
| Ci-1-11A | | 16 | 31 | | 25 | | 28 |
| Al-augite Group | | | | | | | |
| Ci-9-80 | | | 75 | 21 | 1 | | 3 |
| Ki-2-28 | 4 | | 55 | 15 | 23 | | 3 |
| Ki-5-88 | 5 | | 29 | 9 | 35 | | 22 |
| Ki-5-241 | 11 | | 26 | 5 | 35 | | 23 |
| Unclassified[2] | | | | | | | |
| Ci-1-402 | 73 | 10 | 1 | 1 | | 4 | 11 |

[1] Ki-5-31, peridotite; Ki-5-17, olivine websterite; Ci-1-544A, phlogopite, amphibole clinopyroxenite; Ci-1-281, amphibole peridotite; Ki-5-139, plagioclase peridotite; Ki-5-229, mafic gabbro; Ki-5-47, gabbro; Ci-1-265, gabbro; Ci-6-2, olivine gabbro; Ci-1-2C, gabbro; Ci-1-11A, gabbro; Ci-9-80, plagioclase-bearing clinopyroxenite intruded by gabbro; Ki-2-28, gabbro; Ki-5-88, olivine microgabbro; Ki-5-241, olivine microgabbro

[2] Ci-1-402, infiltrated host peridotite of plagioclase hornblendite vein